

A Low-Cost Dual-Band RF Power Amplifier for Wireless Communication Systems

Duy Manh LUONG¹, Quang Kien TRINH¹, Thi Anh NGUYEN²

¹ Dept. of Radioelectronic Engineering, Le Quy Don Technical University, Hoang Quoc Viet Street 236, Hanoi, Vietnam

² Viettel Aerospace Institute, Viettel Building - Hoa Lac Hi-Tech Park, Tan Xa, Thach That, Hanoi, Vietnam

manhld@lqdtu.edu.vn

Submitted July 22, 2022 / Accepted December 19, 2022 / Online first February 27, 2023

Abstract. This paper presents a design of a low-cost concurrent dual-band power amplifier operating at 1.8 GHz and 2.6 GHz. The design combines the signal splitting and second harmonic suppression techniques. The power amplifier aims at achieving the high-efficiency while rejecting unwanted output mixing products when operating in the dual-band mode. These advantages are obtained by using a harmonic termination technique combining with a signal splitting method. The designed amplifier is tested at both small- and large-signal performance through simulations and measurements. The designed amplifier delivers 10.2 dB Gain, 41.2 dBm Pout, and PAE of 40.2% at 1.8 GHz and 10.1 dB Gain, 41.1 dBm Pout, and PAE of 38.7% at 2.6 GHz. The second harmonic suppression for 1.8 GHz band is 49 dBc while the second harmonic for the 2.6 GHz is nearly total suppression. In addition, by using the proposed circuit, the unwanted mixing products can be significantly reduced improving linearity performance.

Keywords

Dual-band power amplifier, GaN HEMT, diplexer, harmonic suppression, cross-modulation

1. Introduction

The development of mobile communication systems requires many challenges to the functions of the hardware. One of the important requirements is that the power amplifiers (PAs) operate in multiband. When operating in the multiband mode, one serious problem for the PA is the effect of cross-modulation causing distortion for the output signal, thus degrading the linearity of the PA when using in the next-generation wireless communication systems. This leads to a challenging task when designing the PA working in the wireless systems: it must operate in multiband mode while still ensuring high-efficiency and linearity. Modern techniques such as Doherty [1], [2], Envelope Tracking [3], [4] or Out-phasing [5], [6] have been introduced to overcome these issues.

The Doherty PA (DPA) is designed to optimize linearity and performance simultaneously [7], [8]. The biggest advantage of the DPA is that it offers great efficiency and high linearity in large power back-off. However, the structure of DPA is quite complicated and not really suitable for modulation applications such as FM, FSK, PSK, ... and its bandwidth is limited. An RF power amplifier operates most efficiently when output power starts saturation and Envelope Tracking (ET) power amplifiers take advantage of this feature [9]. The ET amplifier ensures that the amplifier operates as close to the compression point as possible by regulating the voltage supply. This technique has many advantages such as operation with wide bandwidth, high efficiency. Nevertheless, it faces disadvantages including many block components, difficulty to synchronize between the control branch and RF branch, and is only applicable to systems with small peak to average power ratio (PAPR). The Out-phasing PA consists of two single PAs used to amplify two phase-modulated carriers, and at the output, the envelope of the input signal can be recovered with amplified amplitude and high total efficiency [10], [11]. Because after splitting the signal envelope is fixed and its magnitude contains no information, high-efficiency branching amplifiers can be used to obtain high total efficiency and linearity. However, due to the difficulty of designing highly efficient output power combiners, the advantage of performance is sometimes limited. Besides these methods, other solutions for multiband operation of the PA also presented [12–14]. In these works, authors employ the second harmonic termination technique to suppress the second harmonic improving efficiency at the two operation bands. However, despite the great enhancement of efficiency, the linearity including the cross-modulation effect due to the dual-band operation is not mentioned or investigated in these works.

In this paper, a simple method for improving efficiency with good linearity for dual-band PA is presented. First, a signal splitting method is employed to improve the linearity of the dual-band operation by rejecting undesired output mixing products. After that, a second harmonic termination is used for suppressing the second harmonics to improve the efficiency. The proposed circuit configuration is depicted in Fig. 1. A dual-band input signal with frequencies of f_1 and f_2

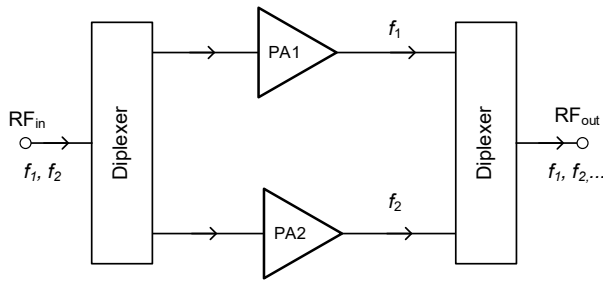


Fig. 1. Block diagram of the dual-band PA using diplexer at both input and output sides.

is split using a diplexer. Each signal will then be input to individual amplifiers which amplify signal of f_1 and f_2 separately.

The intermodulation and cross-modulation distortion components are eliminated by using the diplexer and the second-order harmonics are suppressed by the harmonic suppression circuit embedded in each output matching network of each amplifier, so that the output frequencies of the PA is only the fundamental frequency components. The signal separation technique based on using the diplexer would ideally prevent two different frequencies from being fed into the same active element completely, thereby eliminating intermodulation distortion. At the same time, in each branching power amplifier, the design of the impedance matching circuit and the harmonic suppression circuit is not as complicated as that of the wideband impedance circuits. In this study, this method is applied for the PA fabricated on a FR-4 substrate which is a low-cost single-layer material.

The rest of the paper is organized as follow: Section 2 describes in details the designs of individual components and presents the results of measuring fabricated dual-band PA in comparison with simulation outcomes in software. Section 3 concludes the paper.

2. Design Procedure

2.1 Diplexer

All of diplexer circuits and individual PAs are fabricated on a FR-4 substrate ($\epsilon_r = 4.5$, $\tan\delta = 0.014$, substrate thickness: 0.8 mm, conductor thickness: 35 μm) which is a typical low-cost material.

Figure 2 indicates the schematic of the diplexer. The left arm of the diplexer blocks signal at f_1 and passes the f_2 signal. Similarly, the right arm blocks f_2 signal and passes the f_1 signal. To function such a purpose, in each arm, two quarter-wavelength lines are employed to create open-circuited condition for f_1 and f_2 signals. After that, two stubs l_1 and l_2 are used to make low-impedance condition for f_1 and f_2 signals, respectively. The series quarter-wavelength line at the left arm has the following dimensions: $W = 1.47$ mm, $L = 21.6$ mm; the quarter-wavelength stub at the left arm has the following dimensions: $W = 1.14$ mm, $L = 19.3$ mm; the stub l_1 has the following dimensions: $W = 0.5$ mm, $L =$

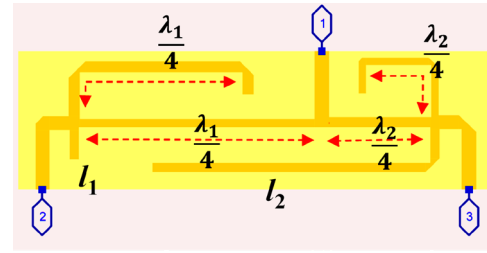


Fig. 2. Schematic of the diplexer.

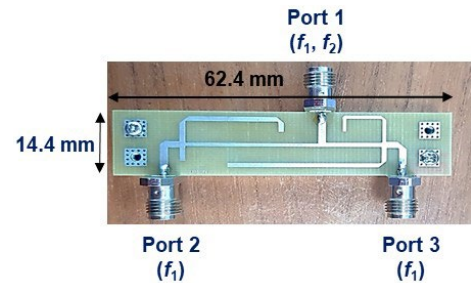


Fig. 3. Fabricated prototype of the diplexer on a low-cost FR-4 substrate.

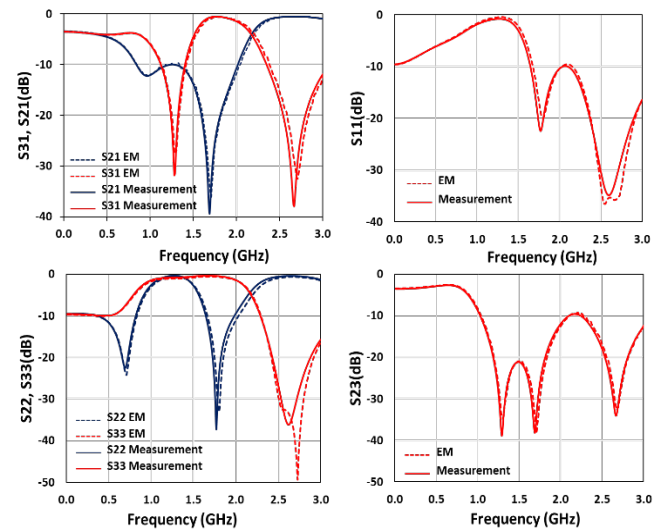


Fig. 4. Simulated and measured results of the S-parameters of the designed diplexer.

2.65 mm. The series quarter-wavelength line at the right arm has the following dimensions: $W = 1.47$ mm, $L = 10.66$ mm; the quarter-wavelength stub at the right arm has the following dimensions: $W = 0.88$ mm, $L = 7.79$ mm; the stub l_2 has the following dimensions: $W = 0.5$ mm, $L = 30.56$ mm.

Figure 3 shows the fabricated prototype of the diplexer on the FR-4 substrate. Two frequencies $f_1 = 1.8$ GHz and $f_2 = 2.6$ GHz are fed into Port 1, and then pass through the blocking blocks which are responsible for transforming the lines from Port 1 to Port 2 and Port 3 into simple 50- Ω lines at f_2, f_1 , respectively thanks to the quarter-wavelength open stubs and their reactance compensation. By adjusting characteristic impedances and electrical lengths of the stubs, transmission and rejection of each frequency band can be realized.

The simulated and measured results of the designed diplexer are shown in Fig. 4. A very good agreements between the simulations and measurements can be observed. The diplexer function is clearly fulfilled and the diplexer has been designed well. The small differences between simulations and measurements are due to the practical loss in connectors and welds, also the loss of FR-4 material. However, the measured results of practical circuit are satisfying the design requirements. In the 1.8 GHz band branch, the measured transmission is -0.6 dB while the measured rejection of 2.6 GHz is -21.8 dB; in the 2.6 GHz band branch, the measured transmission is -0.6 dB while the measured rejection of 1.8 GHz is -21.4 dB. The measured return losses at each port are better than -20 dB while the isolation between output ports is also better than -20 dB.

2.2 Single Amplifier

In this design, the PA operates under a deep class-AB, with drain bias voltage $V_{DS} = 28$ V and gate bias voltage $V_{GS} = 1.94$ V. Each single power amplifier is designed with impedance matching circuits in both source and load sides. Open stubs are employed to terminate the second harmonic by making harmonic impedances close to a purely reactive element. By this way, the second harmonic is suppressed and does not leak to the load. The load/source pull technique is used to determine the optimum impedances of the input and output matching circuit. Block diagram of the single amplifier is described in Fig. 5. At the input matching side, the stub l_{S1} is used to suppress the second harmonic and the stub l_{S2} is used to match the 50Ω to the optimum source impedance at the fundamental frequency. Similarly, at the output side, the stubs l_{L1} and l_{L2} have the same functions as the stubs at the input side.

Figure 6 and Figure 7 show two fabricated single PAs at 1.8 GHz and 2.6 GHz, and the comparison of input/output impedance matching values between electromagnetic (EM) simulation and practical circuit. Dimensions of the stub l_{S1} , l_{S2} and l_{L1} , l_{L2} for the 1.8 GHz and 2.6 GHz amplifiers are given in Tab. 1.

It can be seen that, at fundamental frequencies, the result of the EM simulation and measurement is relatively close, but for the second harmonic, there are small differences between the results due to tolerance in the fabrication process of the PCB. However, the second harmonic impedances are still near the edge of Smith chart indicating a nearly reactive element.

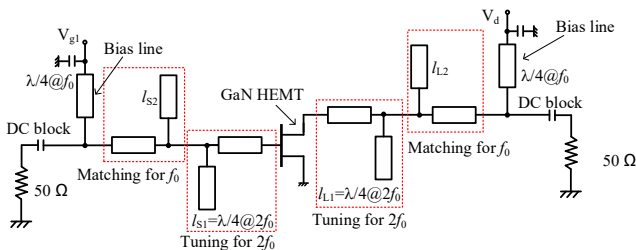


Fig. 5. Block diagram of the single amplifier with input/output matching networks treating up to second harmonic.

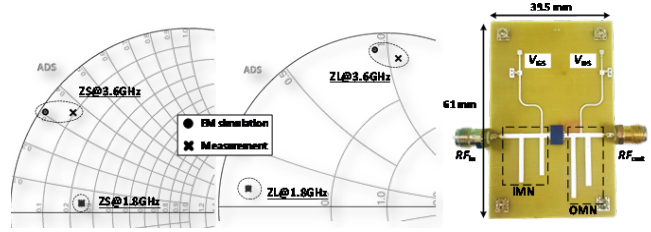


Fig. 6. Simulated and measured impedances and fabricated 1.8-GHz PA.

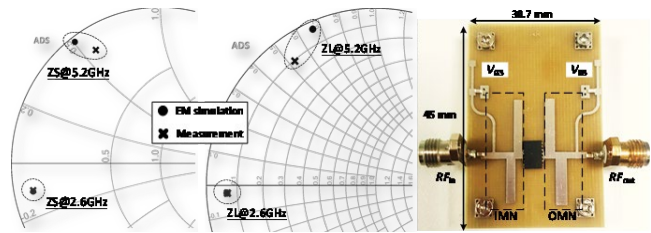


Fig. 7. Simulated and measured impedances and fabricated 2.6-GHz PA.

Amplifier	W/l _{S1}	W/l _{S2}	W/l _{L1}	W/l _{L2}
1.8 GHz PA	1.47/11.39	1.47/12.8	1.5/18.3	1.8/14.7
2.6 GHz PA	1.9/11.64	2/9.53	2.2/11.9	2.5/10

Tab. 1. Stubs dimensions of each single amplifier (in mm).

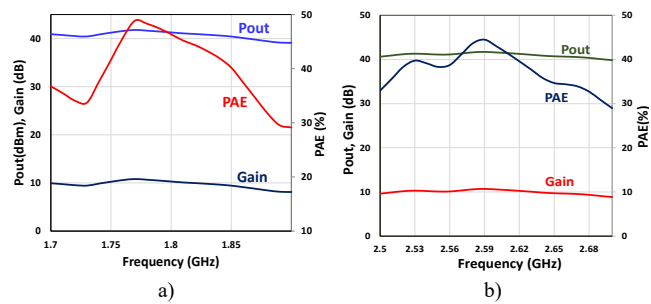


Fig. 8. The frequency response of the large-signal parameters of: (a) 1.8-GHz PA and (b) 2.6-GHz PA.

Figure 8 shows the response of parameters including PAE, Gain, Pout of fabricated PAs with frequency. For the 1.8-GHz PA, the maximum PAE is 49% with Gain of 10.1 dB, and Pout of 42.1 dBm at 1.77 GHz. For the 2.6-GHz PA, the above parameters are 44.5%, 10.7 dB, and 41.7 dBm at 2.59 GHz, respectively.

2.3 Dual-Band PA

The dual-band PA is constructed by connecting input/output diplexers with single PAs designed previously. Figure 9 shows the photograph of the fabricated dual-band PA prototype. The entire circuit size is 5.48 cm \times 10.44 cm.

Figure 10 describes the experimental setup for small-signal measurement. The small-signal performance is measured using a vector network analyzer N5242A from Keysight. The measured results are shown in Fig. 11.

It is noticeable that there are relatively great similarities between the results of EM simulation and measurement at the design bands. At 1.8 GHz and 2.6 GHz, Gain is

10.7 dB and 9.5 dB respectively. By using the setup shown in Fig. 12 and Fig. 13, the large-signal parameters are tested and measured.

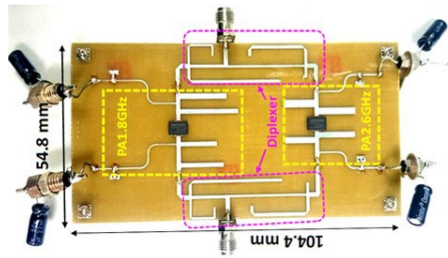


Fig. 9. The fabricated dual-band PA prototype incorporating diplexer and two single amplifiers.

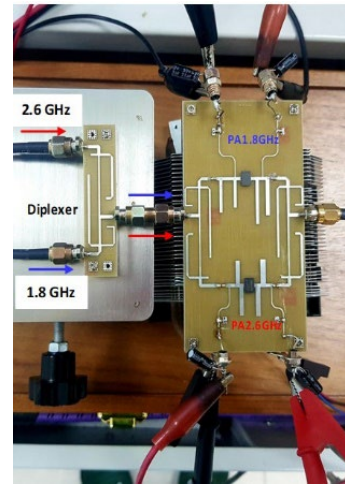


Fig. 13. Connection at the dual-band PA part with an additional diplexer at the input to combine two input signals at 1.8 GHz and 2.6 GHz.

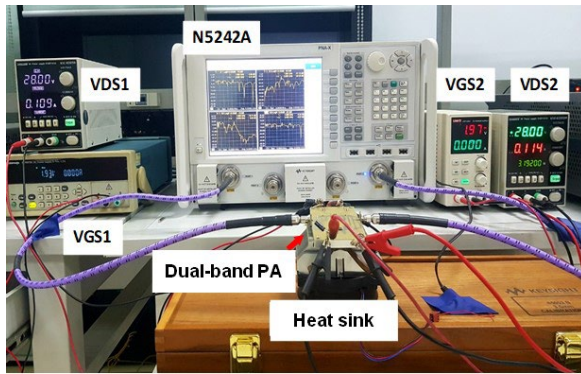


Fig. 10. Small-signal measurement setup using a vector network analyzer (N5242A) from Keysight.

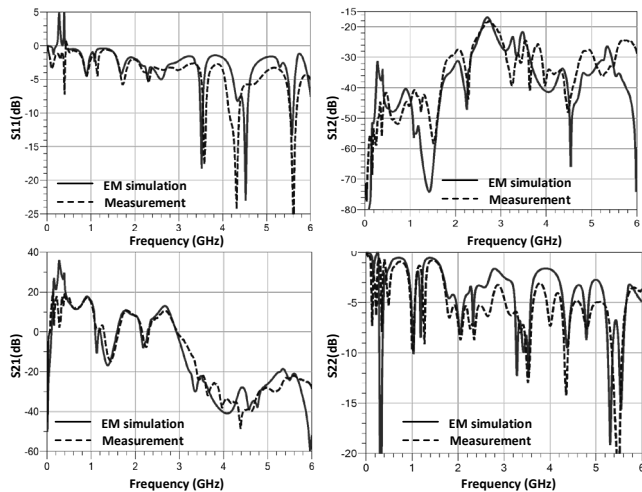


Fig. 11. Measured small-signal performance of the designed dual-band PA.

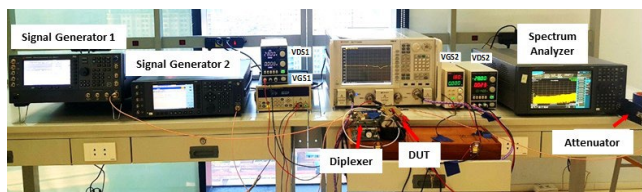


Fig. 12. Large-signal measurement setup for the designed dual-band PA.

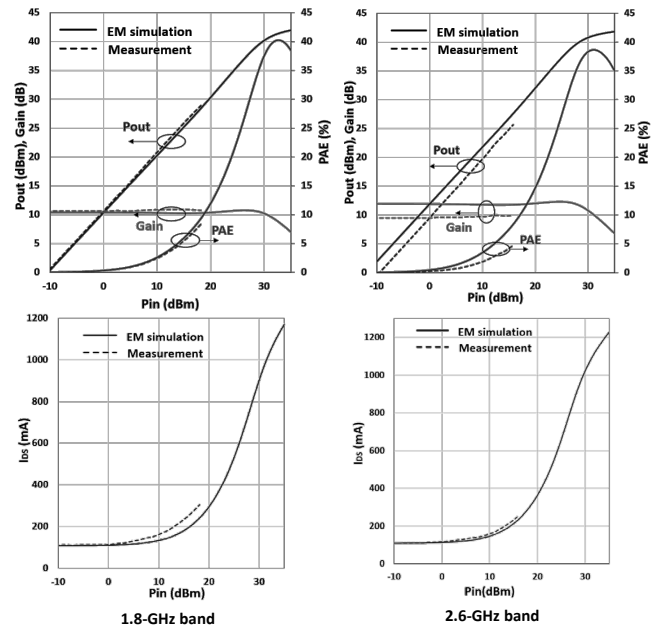


Fig. 14. Simulated and measured transfer characteristics (upper) and drain current characteristics (lower).

In this setup, two signal generators are connected to the input diplexer to input RF dual-band signal to the PA. The PA output is terminated by a spectrum analyzer to display output spectrum. A limit of measuring process is that the RF signal transmitter in laboratory only releases the maximum input of 20 dBm, so parameters of large-signal measurement are only presented and calculated in 10-dBm to 20-dBm range of Pin.

The large-signal characteristics of the designed PA including PAE, output power (Pout) and Gain, drain current Ids are given in Fig. 14.

Although the measured results are not presented fully, they agree well with the simulation. At high frequencies, the loss of FR-4 material makes Pout decrease that results in reduction of Gain and PAE at higher frequency.

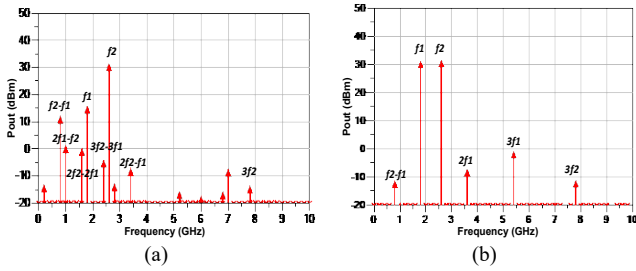


Fig. 15. Simulated output spectrum of: a) single PA, b) designed dual-band PA.

Finally, the linearity in term of harmonic and unwanted mixing products rejection of the designed PA has been investigated to validate the proposed method. Figure 15 shows the comparison between the simulated results for the output spectrum of the single PA and the designed dual-band PA. It is clearly seen a cleaner output spectrum of the dual-band PA thanks to the signal splitting method and second harmonic termination circuits.

These results are compared with the experiment as shown in Fig. 14. The figure describes the measured spectrum of the designed dual-band PA. It shows that the PA itself removed several high-order and unwanted intermodulation distortion components. Importantly, the ability of suppressing harmonic is presented well through second harmonic suppression at 1.8 GHz of 49 dBc, at 2.6 GHz this was too small to observe on the spectrum analyzer. This is due to the highly efficient second harmonic control circuit

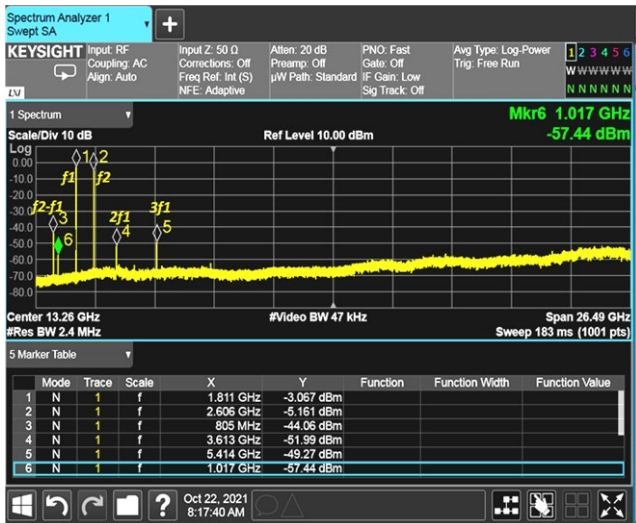


Fig. 16. Measured output spectrum of the designed dual-band PA on a spectrum analyzer from Keysight.

Spurious rejection	Single PA (Simulated)	Dual-band PA (Measured)
$P_{out}(f_2 - f_1) - P_{out}(f_1)$	-4 dBc	-41 dBc
$P_{out}(2f_1 - f_2) - P_{out}(f_1)$	-15 dBc	-54 dBc
$P_{out}(2f_1) - P_{out}(f_1)$	$-\infty$ dBc	-49 dBc
$P_{out}(2f_2) - P_{out}(f_1)$	-20 dBc	$-\infty$ dBc
$P_{out}(3f_1) - P_{out}(f_1)$	-30 dBc	-46 dBc

Tab. 2. Spurious rejection of the proposed dual-band PA.

Ref.	Frequency (GHz) f_1/f_2	PAE (%) @ f_1/f_2	Pout (dBm) @ f_1/f_2	Gain (dB) @ f_1/f_2	Spurious rejection (dBc)
[13]	1.4/2.4	65/65	41/40	13/12.5	N/A
[15]	1.9/2.6	72/66	41.1/40.8	10/10	N/A
[16]	1.5/3.8	47/52	37.3/35.7	15/10	N/A
[17]	4.5/8.5	61/64	32/37	11/9	-41@ $(3f_1 - f_2)$; -41@ $2f_1$
This work	1.8/2.6	40.2/38.7	41.2/41.1	10.2/10.1	-49@ $2f_2$; $-\infty$ @ $2f_1$; -41@ $(f_2 - f_1)$; -54@ $(2f_1 - f_2)$; -46@ $3f_1$

Tab. 3. Comparison between the proposed PA and other works.

incorporated in each PA. The measured spectrum in Fig. 16 is also highly consistent with the simulated spectrum shown in Fig. 15(b).

Table 2 shows the spurious rejection of the designed dual-band PA in comparison with the single PA. The measured spurious rejection has confirmed that the designed PA can remove significantly undesired mixing signal products at the output of the PA. These results have validated the accuracy of the method.

Performance summary and comparison with the other concurrent dual-band amplifiers are listed in Tab. 3. From the comparison, although the PA was implemented in a low-cost FR-4 substrate, thanks to the proposed method good performances could be obtained, especially in efficiency and linearity in term of the spurious rejection.

3. Conclusions

This paper presents a design of a low-cost dual-band PA operating at 1.8 GHz and 2.6 GHz. By splitting input dual-band signal into single frequency components fed to a low-loss and high-isolation diplexer and amplified in single PAs and applying the second harmonic suppression technique, the proposed PA achieved a high-efficiency while still retained the linearity when operating in the multiband mode. The designed amplifier is fabricated and tested at both small and large signal performance. The amplifier delivers a Gain of 10.2 dB, Pout of 41.2 dBm, and PAE of 40.2% at 1.8 GHz and Gain of 10.1 dB, Pout of 41.1 dBm, and PAE of 38.7% at 2.6 GHz. The second harmonic suppression for 1.8 GHz band is 49 dBc while the second harmonic for the 2.6 GHz is nearly total suppression. Moreover, by using the proposed circuit, the unwanted mixing products at the output can be significantly reduced. With these advantages, the designed PA can become a promising candidate for using in the next-generation wireless communication systems.

References

[1] DOHERTY, W. A new high-efficiency power amplifier for modulated waves. *Proceedings of the Institute of Radio Engineers*, 1936, vol. 24, no. 9, p. 1163-1182. DOI: 10.1109/JRPROC.1936.228468

- [2] KIM, B., KIM, J., KIM, I., et al. The Doherty power amplifier. *IEEE Microwave Magazine*, 2006, vol. 7, no. 5, p. 42–50. DOI: 10.1109/MW-M.2006.247914
- [3] RAAB, F., ASBECK, P., CRIPPS, S., et al. Power amplifiers and transmitters for RF and microwave. *IEEE Transactions on Microwave Theory and Technique*, 2002, vol. 50, no. 3, p. 814–826. DOI: 10.1109/22.989965
- [4] STAUDINGER, J., GILSDORF, B., NEWMAN, D., et al. High efficiency CDMA RF power amplifier using dynamic envelope tracking technique. In *2000 IEEE MTT-S International Microwave Symposium Digest*. Boston (MA, USA), 2000, p. 873–876. DOI: 10.1109/MWSYM.2000.863319
- [5] RAAB, F. Efficiency of outphasing RF power-amplifier systems. *IEEE Transactions on Communications*, 1985, vol. 33, no. 10, p. 1094–1099. DOI: 10.1109/TCOM.1985.1096219
- [6] BARTON, T. Not just a phase: Outphasing power amplifiers. *IEEE Microwave Magazine*, 2016, vol. 17, no. 2, p. 18–31. DOI: 10.1109/MMM.2015.2498078
- [7] LIU, M., GOLESTANEH, H., BOUMAIZA, S. A concurrent 2.15/3.4 GHz dual-band Doherty power amplifier with extended fractional bandwidth. In *IEEE MTT-S International Microwave Symposium (IMS)*. San Francisco (CA, USA), 2016, p. 1–3. DOI: 10.1109/MWSYM.2016.7540189
- [8] YIN, Y., XIONG, L., ZHU, Y., et al. A compact dual-band digital Doherty power amplifier using parallel-combining transformer for cellular NB-IoT applications. In *IEEE International Solid-State Circuits Conference (ISSCC)*. San Francisco (CA, USA), 2018, p. 408–410. DOI: 10.1109/ISSCC.2018.8310357
- [9] SARBISHAEI, H., HU, Y., FEHRI, B., et al. Concurrent dual-band envelope tracking power amplifier for carrier aggregated systems. In *IEEE MTT-S International Microwave Symposium (IMS2014)*. Tampa (FL, USA), 2014, p. 1–4. DOI: 10.1109/MWSYM.2014.6848539
- [10] PEDNEKAR, P. H., BARTON, T. W. Dual-band Chireix combining network. In *IEEE Texas Symposium on Wireless and Microwave Circuits and Systems (WMCs)*. Waco (TX, USA), 2016, p. 1–4. DOI: 10.1109/WMCs.2016.7577486
- [11] RUIZ, M. N., MORANTE, R., RIZO, L., et al. A dual-band outphasing transmitter using broadband class E power amplifiers. In *International Workshop on Integrated Nonlinear Microwave and Millimetre-wave Circuits (INMMiC)*. Leuven (Belgium), 2014, p. 1–3. DOI: 10.1109/INMMiC.2014.6815087
- [12] ENOMOTO, J., ISHIKAWA, R., HONJO, K. A 2.1/2.6 GHz dual-band high-efficiency GaN HEMT amplifier with harmonic reactive terminations. In *9th European Microwave Integrated Circuit Conference*. Rome (Italy), 2014, p. 544–547. DOI: 10.1109/EuMIC.2014.6997914
- [13] MENG, X., YU, C., WU, Y., et al. Design of dual-band high-efficiency power amplifiers based on compact broadband matching networks. *IEEE Microwave and Wireless Components Letters*, 2018, vol. 28, no. 2, p. 162–164. DOI: 10.1109/LMWC.2017.2787058
- [14] CAI, Q., CHE, W., MA, K., et al. A concurrent dual-band high-efficiency power amplifier with a novel harmonic control network. *IEEE Microwave and Wireless Components Letters*, 2018, vol. 28, no. 10, p. 918–920. DOI: 10.1109/LMWC.2018.2860798
- [15] PANG, J., HE, S., HUANG, C., et al. A novel design of concurrent dual-band high efficiency power amplifiers with harmonic control circuits. *IEEE Microwave and Wireless Components Letters*, 2016, vol. 26, no. 2, p. 137–139. DOI: 10.1109/LMWC.2016.2517334
- [16] LIU, R., SCHREURS, D., RAEDT, W. D., et al. Concurrent dual-band power amplifier with different operation modes. In *2011 IEEE MTT-S International Microwave Symposium*. Baltimore (MD, USA), 2011, p. 1–3. DOI: 10.1109/MWSYM.2011.5973222
- [17] NISHIZAWA, H., TAKAYAMA, Y., ISHIKAWA, R., et al. Anti-interference circuit configuration for concurrent dual band operation in high-efficiency GaN HEMT power amplifier. *Progress In Electromagnetics Research C*, 2019, vol. 93, p. 199–209. DOI: 10.2528/PIERC19041302

About the Authors ...

Duy Manh LUONG (corresponding author) was born in Son La, Vietnam. He received the B.S. and M.S. degrees in Physics from the Hanoi University of Science (HUS), a member of the Vietnam National University (VNU), Hanoi, Vietnam, in 2005 and 2007, respectively, and the D.E. degree in Electronics Engineering from the University of Electro-Communications (UEC), Tokyo, Japan, in March 2016. He worked at the Graduate School of Engineering Science, Osaka University, Japan as a postdoctoral researcher from April 2016 to June 2017. He is currently Deputy Head of the Department of Wireless Technology, Faculty of Radio-Electronic Engineering, Le Quy Don Technical University, Hanoi, Vietnam. His research interests include development of microwave semiconductor devices and circuits and terahertz (THz) integrated systems for wireless communication applications based on resonant tunneling diodes (RTDs) and photonic crystals.

Quang Kien TRINH (Member, IEEE) received the B.S. and M.S. degrees in Applied Mathematics and Physics from the Institute of Physics and Technologies (State University), Moscow, Russia, in 2007 and 2009, respectively, and the Ph.D. degree in Computer Engineering from the National University of Singapore, in 2018. He is currently a Senior Researcher and the Deputy Head of the Department of Microprocessor Engineering, Faculty of Radio-Electronics, Le Quy Don Technical University. He has authored or coauthored more than 35 publications. His research interests include low-power integrated circuit design, emerging memory technologies, and hardware security.

Thi Anh NGUYEN received the B.S. degrees in Electronics Engineering from Le Quy Don Technical University, Hanoi, Vietnam in 2021. She is currently a technical staff at the Viettel Aerospace Institute, Hanoi, Vietnam. Her research interests include development of microwave semiconductor circuits and modules for wireless communications.